European Polymer Journal 188 (2023) 111933

Contents lists available at ScienceDirect

European Polymer Journal

journal homepage: www.elsevier.com/locate/europolj

Development of self-healing vanillin/PEI hydrogels for tissue engineering

Merve Yasar [a], Burcu Oktay [b], Fulya Dal Yontem [c], Ebru Haciosmanoglu Aldogan [d], Nilhan Kayaman Apohan [b,*]

[a] Marmara University, Institute of Pure and Applied Sciences, Department of Chemistry, 34720 Goztepe, Kadikoy, Turkey
[b] Marmara University, Faculty of Science, Department of Chemistry, 34722 Goztepe, Istanbul, Turkey
[c] Koç University, Koç University School of Medicine, Department of Biophysics, 34450 Sariyer, Istanbul, Turkey
[d] Bezmialem Vakif University, Faculty of Medicine, Department of Biophysics, Fatih, 34093 Istanbul, Turkey

ARTICLE INFO

Keywords:
Hydrogels
Self-healing
UV-polymerization
Vanillin

ABSTRACT

Self-healing materials recover mechanical damages to expand the lifetime of the material provided. In this study, self-healing hydrogels have been successfully prepared using a novel and simple technique. Vanillin is a natural monomer, used as a bio-based cross-linker for UV-induced bonding and Schiff-base bonding. Methacrylate-functionalized vanillin (M-VAN) is covalently integrated with the polymer matrix. While M-VAN supports polymer matrix with its vinyl group, its aldehyde functionality helps the formation of dynamic covalent imine bonds via Schiff-base formation. The hydrogel showed excellent self-healing ability overnight under physiological conditions without external addition. In addition, the hydrogel surface was modified by collagen and its cell viability was investigated. The prepared scaffolds showed good cell viability of 124% and 163% compared to the control sample. The developed self-healing material reveals that it has possible uses for future biomedical applications and tissue engineering studies due to the self-healing mechanism taking place under ambient conditions.

1. Introduction

Hydrogels occurred by three-dimensional (3D) arrangement of polymer chains through physical or chemical interactions. Hydrogels are the ideal support for biomedical applications because of their biocompatibility and biodegradability [1]. In addition, their water retention capability and porosity cause high swelling in aqueous solutions. However, poor mechanical properties of the hydrogel restrict its usage, and efforts to improve the mechanical stability by increasing the irreversible covalent crosslinking make the hydrogel too rigid [2].

Recently, a remarkable number of articles demonstrate that dynamic covalent bonds allow the repair of the material after a break [3–5]. Hydrogels are considered dynamic adaptable materials under physiological conditions. The use of adaptable hydrogels with reversible linkages in wound treatments is advantageous because it reduces the risk of infection by covering deep or irregular wounds [6]. Moreover, its dynamic covalent bonds repair damage in the hydrogel after being destroyed by external mechanical forces [7]. Therefore, it is desirable to use hydrogel with self-healing capabilities.

However, adaptable hydrogels often have poor mechanical properties and a fast erosion rate. Therefore, the integration of a stable covalent network such as an interpenetrating network, nanocomposite network, or double network into an adaptable network is required [8]. Especially, interpenetrating networks provide excellent toughness and fracture strength [9]. Recent developments include the creation of double-network hydrogels, which feature two interpenetrating networks, to enhance the mechanical properties of smart hydrogels [10,11].

Self-healing is an autonomous reaction to heal injury caused by external effects in living systems [12]. Self-repairing of the mechanical damage in polymeric systems is very important, just like the living systems, to increase their lifespan [13]. Initially, this fascinating feature was only used in the automotive sector and industrial fields [14–18]. Nowadays, there has been a long-standing interest in self-healing hydrogels in biomedical applications such as drug delivery, tissue engineering, and strain sensors [19–21].

Self-healing occurs from two different pathways as extrinsic and intrinsic characteristics. In the extrinsic one, self-healing agents are constrained in the polymer matrix. The healing agent is released when the crack ruptured and catalyzes the reaction to activate healing [22]. In

* Corresponding author at: Marmara University, Faculty of Science, Department of Chemistry, 34722 Goztepe-Istanbul, Turkey.
E-mail address: napohan@marmara.edu.tr (N. Kayaman Apohan).

https://doi.org/10.1016/j.eurpolymj.2023.111933
Received 5 December 2022; Received in revised form 8 February 2023; Accepted 13 February 2023
Available online 17 February 2023

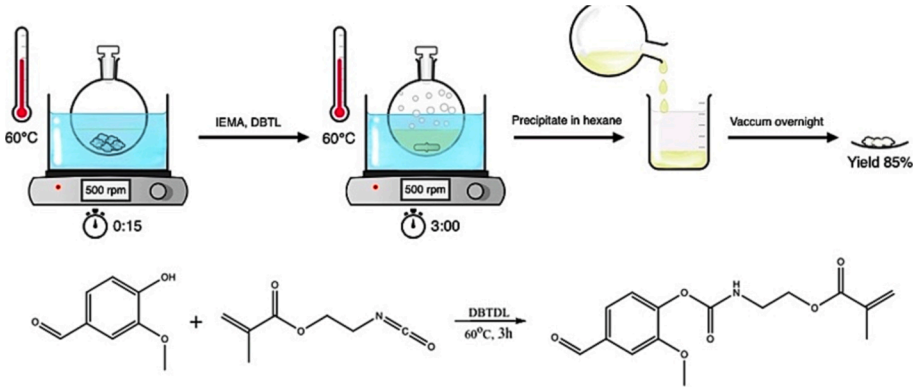

Scheme 1. Synthesis of M-VAN.

intrinsic self-healing, non-covalent bonds such as ionic interactions, hydrophobic interactions, metal–ligand interactions and covalent bonds such as Diel-Alder reactions, disulfides, acyl hydrazones, and Schiff-base take place to bring about self-healing [23–30]. Schiff-base linkages between the amine group and aldehyde group have the advantages of fast reaction speed and mild reaction conditions, which are appropriate for tissue engineering [31,32]. Oxidized hyaluronate and dialdehyde-modified hyaluronic acid-based polymers have been used in previous studies for Schiff-based dynamic bonds. However, the previously reported studies based on Schiff-based dynamic bonds demonstrated that the rigidity of polymer backbone, insufficient imine bond, and multistep reactions fail the self-healing and limit the usage of material [33,34]. To overcome this problem, multiple networks composed of the borate ester bond, Schiff-base, and host–guest interaction were reported. By incorporating these dynamic interactions into polymer hydrogels with good self-healing ability, mechanical strength and stretchability were attained [35–37].

Vanillin (4-hydroxy-3-methoxy benzaldehyde) which is extracted from natural resources can be used as a monomer for sustainable purposes. The aldehyde and hydroxyl reactive groups of vanillin can be used in chemical modifications to produce various polymeric materials [38]. Vanillin-based dynamic covalent bond studies are limited and mechanical properties and self-healing ability still need improvement [39,40]. Lin et al. reported that the concentration of vanillin was critical to the self-healing capability for the vanillin-chitosan hydrogels [24]. Hunger et al. shows that a two-time increase of vanillin improves the compression strength of the samples and led to slower biodegradability [41]. The multiple aldehyde groups containing crosslinkers make the Schiff base interactions stronger [42].

Recent studies in Schiff-base self-healing materials mainly focused on oxidative cleavage of vicinal diols of polysaccharides with sodium periodate, and conjugation of aldehyde-functionalized molecules such as 4-formylbenzoic acid to polymers [43]. In each of these methods, it is inevitable that the structural properties of the polymer are compromised or that impurities from multi-step synthesis cannot be ignored. Moreover, the mechanical properties are unsatisfactory since imine-based hydrogels have weaker cross-links. However, the most useful and easiest way to add self-healing properties to a mechanically strong conventional hydrogel without sacrificing these properties is to use vanillin methacrylate monomer, which can be synthesized in one step. Therefore, in this work, the methacrylate-functionalized vanillin (M−VAN) was synthesized by using a simple and efficient technique. The solubility of M−VAN in ethanol provides an advantage in terms of easy reaction. In addition, M−VAN not only contributes to the formation of Schiff-base for a dynamic reversible bond like other aldehyde sources; but also takes part in the formation of a strong polymer chain by radical polymerization. It has been reported previously that, the gels prepared by in situ radical polymerization following imine formation are tougher and have better self-healing properties than their counterparts containing only imine bonds [44]. Here, the novel hydrogels were prepared by Schiff-base reaction and in situ UV-initiated polymerization techniques. PEI not only formed dynamic imine bonds with M−VAN with its amine functional groups but also contributed to the mechanical strength of the hydrogel. Simultaneously, the stable covalent network was created through chain polymerization by photocuring. While the strong covalent connections enhanced the mechanical properties of the hydrogels, the functional side groups of the monomers (or oligomers) give an extra H-bonding to help self-healing. The self-healing ability of the adaptable hydrogels under physiological conditions makes them a good candidate for several potential uses.

2. Experimental

2.1. Materials

Vanillin (99%) was kindly gifted from AROMSA, TÜRKİYE. Dibutyltin dilaurate (DBTL) (95%) and fumaric acid (FA) (99%) were purchased from Merck. Isocyanato ethyl methacrylate (IEMA) (98%), Poly (ethylene glycol) diacrylate (PEGDA, Mn:700), 2-hydroxy-2methylpropiophenone, 2-hydroxy-2-methylpropiophenone (Darocur1173) (97%) were purchased from Sigma Aldrich. Polyethylenimine branched (PEI) (30 % w/v aqueous solution, MW average: 50.000–100.000 g/mol) was obtained from Polysciences, Inc. Collagen Type I (95%) from bovine tendon was kindly gifted from BUGAMED Biotechnology, TÜRKİYE.

2.2. Characterizations

M-VAN and the hydrogels were characterized by Fourier-Transform Infrared Spectroscopy (FT-IR) using Perkin Elmer ATR-FT-IR Spectrometer. The samples were recorded directly in the range from 4000 to 600 cm^{-1}. The structure of M-VAN was verified by Varian Gemini 400 MHz Proton Nuclear Magnetic Resonance Spectroscopy (^{1}H NMR) using deuterated chloroform.

Differential scanning calorimetry (DSC) was performed using Perkin Elmer Diamond DSC. The hydrogels were soaked in distilled water overnight to remove impurities and dried in an oven for two days until a constant weight was obtained. The first run was performed from −50 to 70 °C and the second run was carried out from −50 to 200 °C with a heating rate of 10 °C/min.

The tensile tests were proceeded using Zwick Z010 Universal Tensile Test Machine at a fixed crosshead speed of 10 mm/min^{-1} at room temperature. The samples were prepared in rectangular shape with dimension of 50x5x1 mm. The test was repeated for at least 3 times.

SEM imaging of hydrogels were performed by using Philips XL30 ESEM-FEG/EDAX North Billerica, MA.

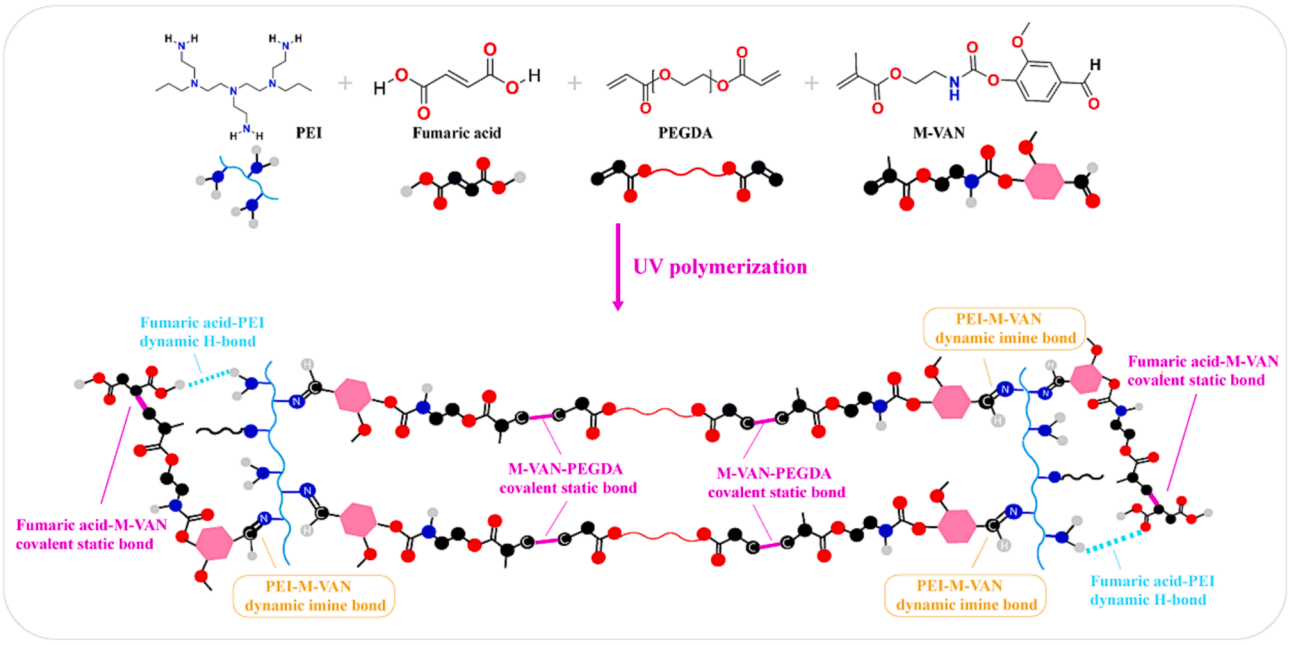

Scheme 2. Hydrogel preparation.

Table 1
Composition and gel contents of hydrogels.

Samples	M-VAN (g)	PEI (g)	PEGDA (g)	Fumaric acid (g)	Gel Content (%)
A0	0.3	0.013	0.2	0.1	88.5
A2	0.3	0.013	0.2	0.3	91.8
A4	0.3	0.03	0.2	0.1	93.7
A6	0.4	0.013	0.2	0.1	94.6
A8	0.3	0.013	0.25	0.1	92.6

2.3. Synthesis of methacrylated-vanillin (M-VAN)

M-VAN was prepared by the reaction of vanillin and IEMA. Firstly, vanillin (1 g; 6.5 mmol) was dissolved in 10 mL of toluene at 60 °C. Then, excess amount of IEMA was incorporated dropwise into the vanillin mixture. DBTL was used as a catalyst. The reaction was stirred for 3 h under N_2 atmosphere. Finally, the mixture was participated in cold hexane to remove un-reacted IEMA. The product was vacuum dried 30 °C for 2 days. The yield was 85%. The reaction scheme is shown in Scheme 1.

2.4. Synthesis of hydrogels

Hydrogel samples were prepared by photopolymerization of M-VAN, fumaric acid, PEGDA-700, and PEI (Scheme 2). Firstly, M-VAN was dissolved in 4.5 mL of ethanol. Then, fumaric acid, PEGDA-700, and PEI (for Schiff-base formation) were added to the solution. Photoinitiator (Darocur 1173) was added and the mixture was vortex for 1 min. Afterwards, the solution was transferred to the plastic tube. Reactions occurred in the UV reactor for 15 min under room temperature. The composition of hydrogels were shown in Table 1.

2.5. Gel content, porosity test and swelling behaviors

Hydrogel samples of about 0.05 g were dried in freeze-drier overnight and weighted (W_d) to determine the gel content. The dried hydrogels were then soaked into deionized water at room temperature overnight to remove uncrosslinked parts. The samples were dried in freeze-drier and weighted (W_g). The gel content was calculated from Equation (1):

$$Gel\ \ Content\% = \frac{W_g}{W_d} X100\% \quad (1)$$

Hydrogel samples were cut evenly and weighted as W_1 then soaked into ethanol overnight to determine the porosity of hydrogels. [45]. After excess ethanol was removed by filter paper, hydrogels were weighted as W_2. The porosity was calculated by following Equation (2):

$$Porosity(\%) = \frac{W_2 - W_1}{V\rho} X100\% \quad (2)$$

where V was volume of hydrogels and ρ was the density of ethanol.

Hydrogel samples were soaked in deionized water overnight to remove unreacted monomers. Then lyophilized overnight and weighted dry hydrogel as W_d. Hydrogel samples were plunged in distilled water (5 mL) at room temperature for desired time intervals (5–2880 min) and weighted as W_s. During measurement, excess water was taken away with filter paper. Swelling tests were repeated three times. The swelling ratio was calculated from Equation (3):

$$SR = \frac{W_s - W_d}{W_d} X100\% \quad (3)$$

where SR: Swelling ratio

Hydrogel samples were lyophilized overnight and weighted as Wd. Dried hydrogels were plunged in a buffer solution of pH 2, 4.5, 7, 8, and 10 at room temperature and weighted as Ws in equilibrium to determine swelling behavior in different ph ranges. The swelling ratio was calculated from Equation (3).

2.6. Self-healing efficiency

Self-healing performance was investigated by comparing the tensile strength of hydrogel sample before and after healing. The hydrogel sample was cut into two pieces and re-contact from cutting areas by applying slight handling pressure. Then samples were kept in an oven at 37 °C overnight. The test was repeated at least 3 times. The healing efficiency (SH_{eff}) was defined as the ratio of the tensile strength of healed sample to the original sample.

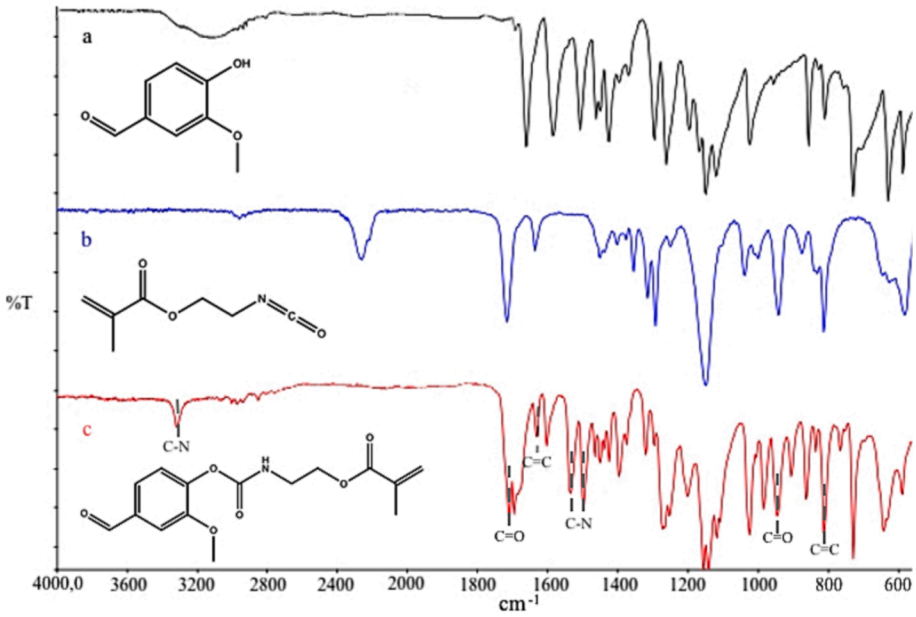

Fig. 1. FT-IR spectra of (a) vanillin, (b) IEMA and (c) M-VAN.

2.7. Cell growth and viability studies

Human fibroblast cells (CCD-1072Sk) were purchased from American Type Culture Collection (ATCC) and maintained in Dulbecco's modified Eagle medium containing 10% fetal bovine serum and 100UI/ml penicillin/streptomycin at 37 °C in a 5% CO_2 incubator. Cell viability was determined using Thiazolyl Blue tetrazolium bromide (MTT) reagent (Alfa Aesar, Thermo Scientific). Collagen-modified scaffolds were prepared by coating the hydrogel surface with 4 μg and 8 μg of Type I collagen dispersed in 0.1 M acetic acid solution, respectively. These scaffolds were then incubated at room temperature for an entire night in a desiccator before being used for cell culture. Afterwards, hydrogels were cut into equal pieces (1 cm × 1 cm) for each well and sterilized under UV for at least 1 h. Cells were seeded into 24 well plates at a density of 5×10^4 cells/well and were incubated with hydrogels for 24 h. At the end of the incubation, hydrogels were removed and MTT reagent was added to each well with a final concentration of 0.1 mg/ml and cells were further incubated for 2 h at 37 °C in a 5% CO_2 incubator until formazan crystals were observed under microscopy. All the media inside the wells were discarded and 300 μl DMSO was added to each well. Absorbance values were read at 570 nm by a Thermo Multiskan GO microplate spectrophotometer (Fisher Scientific). Cell viability was calculated according to Equation (4):

$$CellViability\% = \frac{Meanabsorbanceofthetreatment}{Meanabsorbanceofthecontrol} \text{x}100 \quad (4)$$

Bright field images of the cells were taken by Zeis Axio ZI Invert Microscope.

2.8. Cell fixation

Briefly CCD-1072 Sk cells were seeded into 24 well plates and treated with hydrogels for 24 h. After the incubation, hydrogels were removed from the wells and washed with 1x PBS. The cells attached to the hydrogels were fixed with 1 mL of 2.5 % glutaraldehyde (GA) for 2 h at room temperature. Afterward, hydrogels were washed with 1x PBS for GA removal. Fixated hydrogels were dehydrated by immersing in increasing concentrations of ethanol every ten minutes (50 to 100%, 10% increase at each step). Hydrogels were stored at −20 °C before SEM analysis.

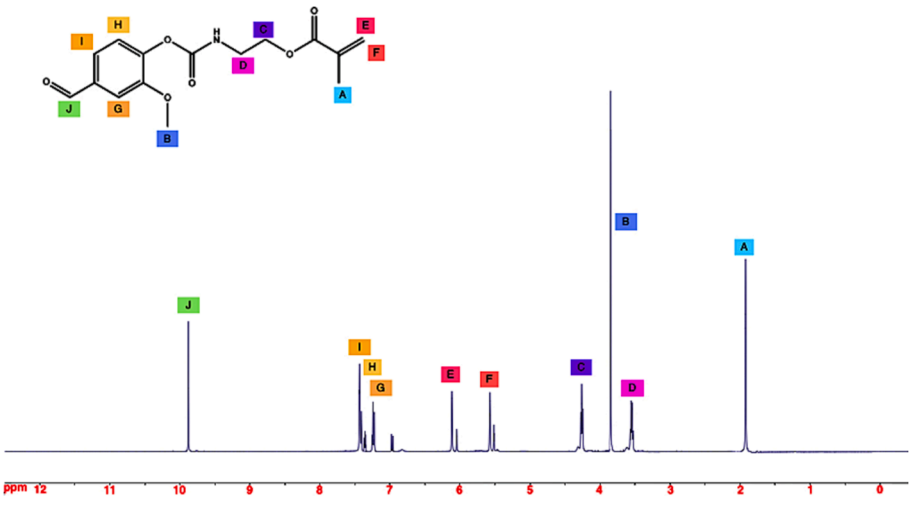

Fig. 2. ^{1}H NMR spectra of M-VAN.

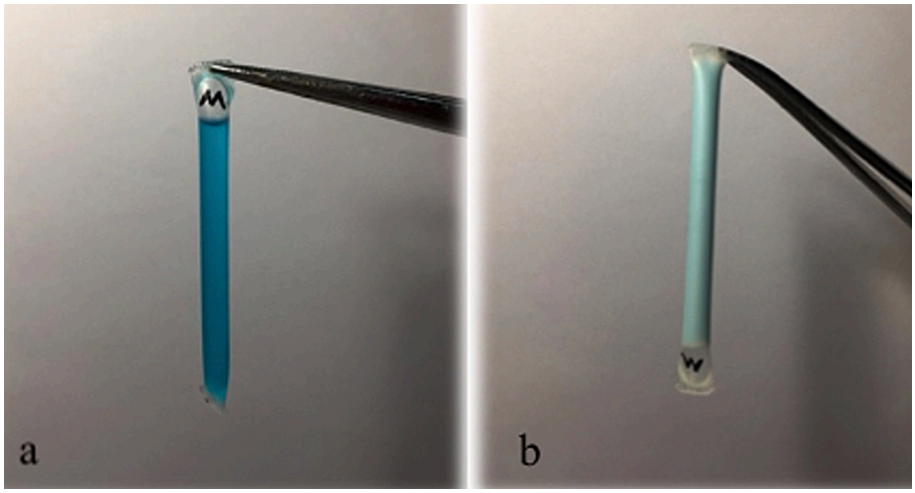

Fig. 3. The left one is initial formulation, the right one is a hydrogel after polymerization.

3. Results and discussions

3.1. Characterization of M-VAN

The aldehyde and hydroxyl functional groups of vanillin make it a suitable compound to undergo several modifications [46,47]. In this study the synthesis of M-VAN was achieved by the reaction between the isocyanate group of IEMA and the hydroxyl group of vanillin to form urethane linkage under inert conditions at 60 °C. It is important to work in a dry atmosphere to prevent the conversion of isocyanate groups to amines. DBTDL catalyzes the reactivity of hydroxyl groups of M-VAN to increase the reaction rate. The product was obtained in a high yield (85%). Unlike methacrylic anhydride counterpart, reaction occur faster without side reaction, giving opportunity to easy extraction in small amounts [48]. Additionally, IEMA exhibits H-bond sources to enhance self-healing capability of material. Above 40 °C in oven M-VAN changes color white to yellowish, hence it should be dried at below 40 °C.

FTIR spectrum of M-VAN was shown in Fig. 1. For comparison the corresponding spectra for vanillin and IEMA was incorporated in the same Fig. As can be seen in Fig. 1a, vanillin has broad hydroxyl (–OH) stretching and bending peaks shown at 3157 cm^{-1} and 1263 cm^{-1} respectively [49]. The aldehyde (C = O) stretching peak is represented at 1662 cm^{-1} [50]. The IR spectrum (Fig. 1b) of IEMA showed the characteristic isocyanate peak (–NCO) at 2261 cm^{-1}.

As can be seen from the IR spectrum (Fig. 1c) of functionalized vanillin, hydroxyl stretching and bending peaks disappeared. The N–H stretching and C-N stretching peaks occurred at 3319 cm^{-1} and 1536 cm^{-1}, 1499 cm^{-1}, respectively [51]. C-NH stretching occurred around 1426 cm^{-1} due to urethane bond formation. The ester (C = O) stretching and bending peaks occurred at 1710 cm^{-1} and 949 cm^{-1}, respectively. The acrylate double bonds assigned at 1633 cm^{-1} and 813 cm^{-1}. Also, the disappearance of the isocyanate peak indicated that the reaction has completed successfully [52].

Fig. 2 shows the H-NMR spectrum of M-VAN. The singlet peak at 1.8 ppm (A) represents of methyl group of methacrylate. The methoxy group attach to benzyl group observed at 3.87 ppm (B). The peaks at 4.3 ppm (C) and 3.6 ppm (D) correspond to ethylene protons. The peak at 4.45 ppm represents triplet of next to ester group. As an evidence of vinyl

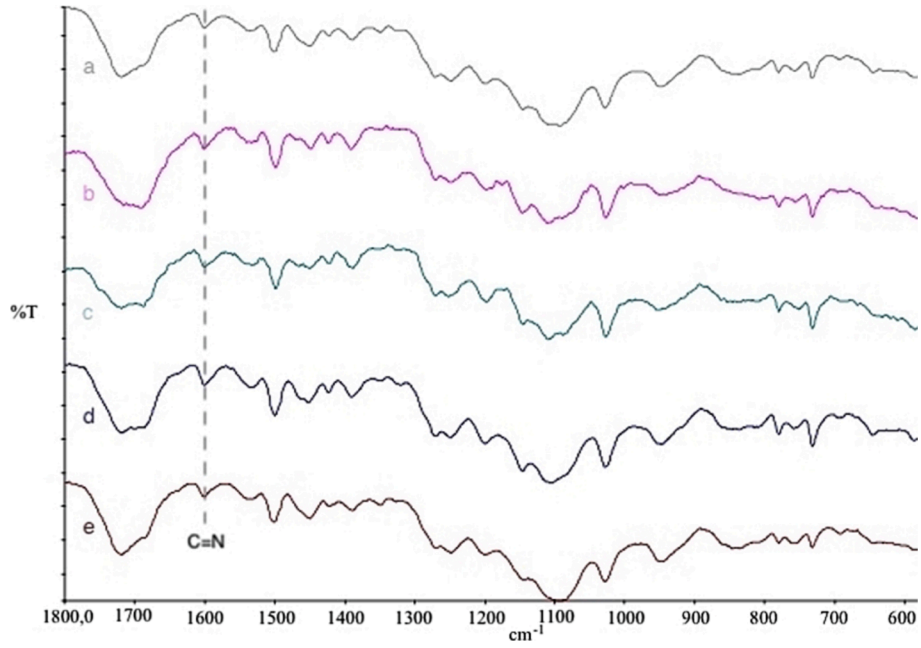

Fig. 4. FTIR spectra of hydrogel samples. a) A0, b) A2, c) A4, d) A6, e) A8.

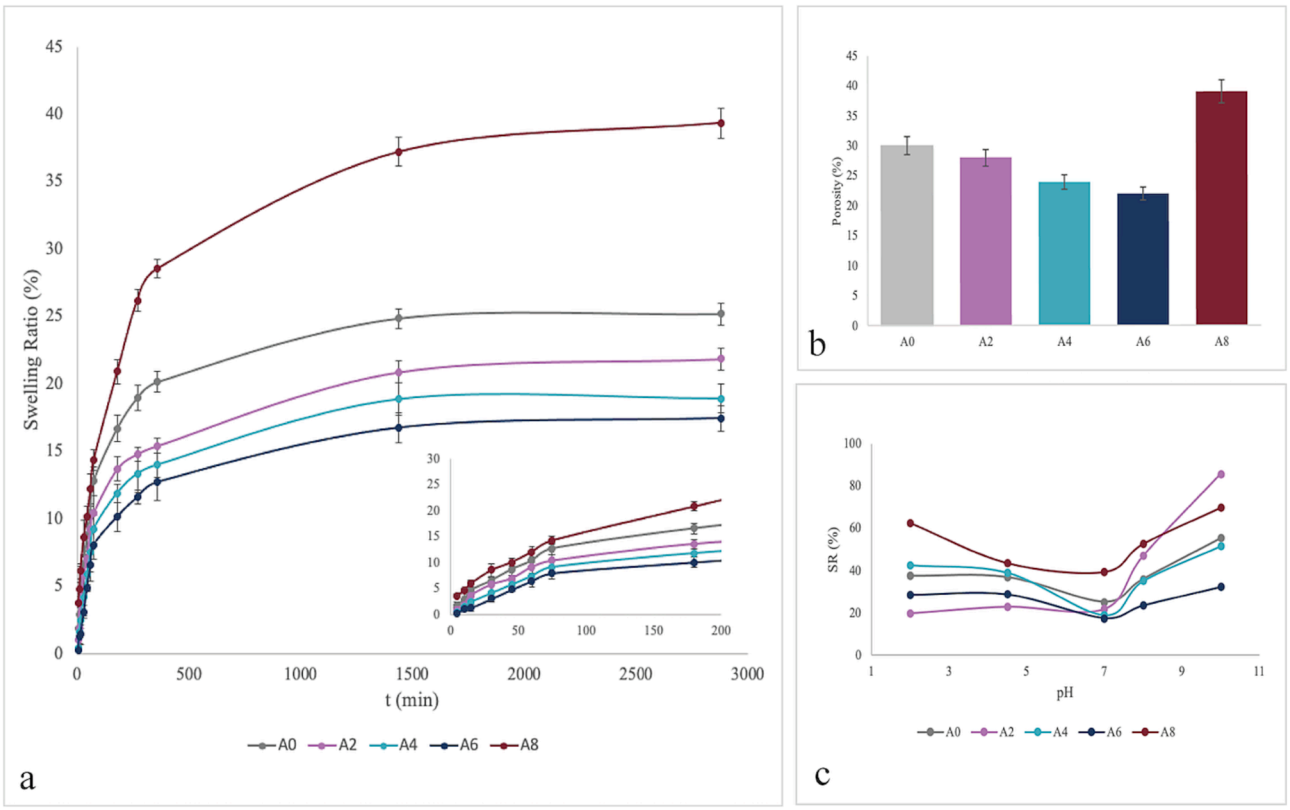

Fig. 5. Swelling behavior and porosity of hydrogel samples a) Swelling ratio, b) Porosity of hydrogels, c) Swelling ability of hydrogels at different pH ranges.

group, the peaks at 6.2 ppm (E) and 5.6 ppm (F) appeared. Around 7.5 ppm (I, H, G) peaks belongs to the protons of aromatic ring. Around 7 ppm peaks belong to solvent. At 9.9 ppm (J) belongs to singlet of aldehyde [53].

3.2. Characterization of vanillin based-hydrogels

As can be seen in Fig. 3, the hydrogels successfully prepared in plastic clear straws with co-polymerization technique under UV irradiation. It took 15 min to complete the reaction. It was observed that during polymerization the hydrogel turns opaque. In Fig. 3, invert tube test method has shown that hydrogel successfully synthesized. The gel contents of hydrogels were found as between 89 and 95%.

Fig. 4 shows the comparative FT-IR spectra of hydrogel samples within the 1800–600 cm^{-1} spectral window. As can be seen, the dried hydrogel showed C=O stretching peak at 1719 cm^{-1}. The disappearance of characteristic acrylate C=C double bond peaks at 1636 cm^{-1} and 813 cm^{-1} showed that the photopolymerization was successfully achieved. In addition, the C=O aldehyde peak of M-VAN at 1662 cm^{-1} disappeared. C-N stretching vibrations at 1450 cm^{-1} and $-NH_2$ scissoring vibration at 1560 cm^{-1} belongs to PEI are disappeared [54–56]. A new C=N stretching peak at 1602 cm^{-1} was observed as an evidence of Schiff-base imine bond between M-VAN and PEI [54–57].

3.3. Swelling behaviors of hydrogels

The equilibrium swelling ratios of the hydrogels were shown in Fig. 5-a. As can be seen, for all hydrogel samples swelling rate increased rapidly up to 80 min. The hydrogel samples reached equilibrium swelling after 24 h. A8 hydrogel sample showed highest swelling ratio amongst all samples. The result indicated that the swelling ratio increases with the amount of PEGDA. The equilibrium swelling ratios seem to decrease with increasing content of M-VAN (A6), PEI (A4). It is probably due to the Schiff-base formation at higher M-VAN and PEI contents, which increases the number of junctions between polymer chains. It is well known that the crosslinking density has an inverse relation with the swelling capacity [58]. In addition, the decrease in swelling ratios of A2 compare to A0 with increasing fumaric acid content may be attributed to possible interpolymer complexes between PEI and FA. The amine groups of PEI can make interaction with the carboxylic groups of fumaric acid. Overall the obtained water swelling ratios are appropriate for tissue engineering applications and wound-repair usage [39].

The porosity of hydrogels were shown in Fig. 5-b. Porosity can be controlled via monomer ratio and preparation conditions. Hydrogel samples showed 22–40% porosity. It might be due to the high polymer density and the crosslinking ratio of the hydrogel. In addition to the covalent crosslink structure of all hydrogels, A4 and A6 samples contain higher Schiff-base linkages as an additional crosslinking point, therefore it decreases the porosity of the structure. In addition, the PEI chain also entangles within the pores of the gel. The porosity of A8 is highest since longer polyether segments of PEGDA decrease crosslinking density of the hydrogel. The porosity results were consistent with the swelling ratios.

Fig. 5-c shows the pH dependence equilibrium swelling ratios of hydrogels. Hydrogel samples showed amphoteric properties due to the presence of acidic groups of fumaric acid as well as amine groups of PEI and M-VAN respectively. At low and high pH levels, the competition between acidic and basic groups is intense due to the amphoteric characteristic of gel. Under acidic conditions, anionic carboxylate and amine groups are protonated. The ionic repulsion of positive charges of ammonium ions create more space for water intake, as we see more obviously in A4. Meanwhile, carboxylic acid groups form hydrogen bonds with one another and with water molecules, limiting the electrostatic repulsion of the carboxylate ion. Dissociation of carboxylic acid groups is negligible until the pKa = 3 is exceeded. Hydrogels showed balance in neutral conditions due to the balance between ionic groups. Higher pH causes carboxylic groups to deprotonate and ionic repulsion

Table 2
Glass transition temperature (Tg) of hydrogels.

Samples	Tg_1	Tg_2
A0	−26	92
A2	–	79
A4	−39	87
A6	–	93
A8	−25	109

creates more space for water intake as we see more obviously in A2. Hydrogels showed slightly higher swelling degrees at alkaline pH than acidic due to the dominant effect of anionic carboxylate ions. Similarly, reported hydrogels were shown higher swelling ability in acidic and basic conditions than in neutral [59–61]. As Schiff-base linkages decomposes in lower and higher pH, reducing crosslink points also enhance swelling capability. Since Schiff base linkages are effective at neutral pH, they cause an increase in crosslink density at pH 7 and decrease the swelling percentage of gels. The pH-dependent swelling test proves the effectiveness of the Schiff base.

3.4. Thermal behaviors of polymers

The DSC thermograms and the glass transition temperatures of hydrogels are shown in Fig S1 and Table 2, respectively. Mainly two Tg was determined for hydrogels. The first Tg (Tg_1) was observed between −39 °C and −25 °C that could be assigned to the thermal transitions of PEI and PEG chains. Since the lowest Tg_1 belongs to A4 sample with higher PEI content, it can be assumed that PEI is the dominant factor with its highly branched structure. It is well known that branching enables polymer chain flow easily due to the increased end groups number and free volume, respectively which leads to reduced Tg [56]. Second Tg (Tg_2) was observed between 79 °C and 109 °C because of the chain polymerization of olefinic monomers. Strong intermolecular forces, steric hindrance and low free volume are responsible for high Tg. The aromatic structure of M-VAN reduces the rotational motion and the carboxylic functionality of fumaric acid increases polar-polar interactions and increases Tg value. In A2 and A6 formulations, higher amount of fumaric acid and M-VAN respectively, may not allowed us to observe Tg_1. Because, styrene-like aromatic group for M-VAN prevents free space and ortho position methoxy group attached to aromatic group increases steric repulsion [62]. For A8 sample, the slight increase in diacrylate content increased Tg_2 because of increasing crosslinked points [63].

3.5. Mechanical behavior of hydrogels

The detailed data for tensile tests are presented in Table 3. The stress–strain curves are also shown in Fig. 6. As can be seen, the hydrogels showed good mechanical strength. Compared to A0, A2 with

Table 3
The mechanical test results for hydrogels.

Samples	Before healing			After healing			
	E-modul (N/mm^2)	Tensile Strength (MPa)	Elongation at break (%)	E-modul (N/mm^2)	Tensile Strength (MPa)	Elongation at break (%)	(SH_{eff}) * (%)
A0	23 ± 1.5	66 ± 2.6	49 ± 1.2	28 ± 1.9	42 ± 2.4	51 ± 1.5	64
A2	33 ± 2.9	47 ± 2	62 ± 3.6	21 ± 3.1	30 ± 4.2	51 ± 2.4	64
A4	24 ± 2.3	62 ± 3.5	54 ± 3.2	13 ± 1.2	39 ± 2.7	51 ± 3.9	63
A6	55 ± 3.6	21 ± 1.5	48 ± 3.1	32 ± 3.5	12 ± 1.3	34 ± 3.4	57
A8	88 ± 4.1	67 ± 3.8	68 ± 4.2	80 ± 3.9	58 + 3.2	46 ± 4.4	87

* Self-healing efficiency SH_{eff}: The ratio of tensile strength of healed sample to the original sample.

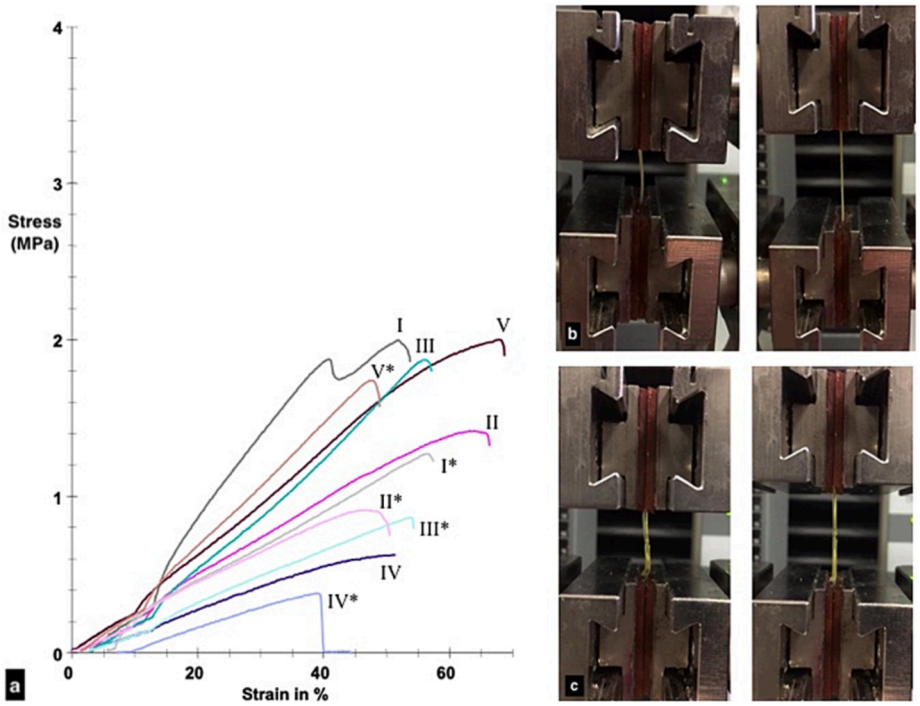

Fig. 6. a) Tensile stress plot; I:A0, II:A2, III:A4, IV:A6, V:A8, *Self-healed. Photographs before and after tensile tests of b) A4 c) Self-healed A4.

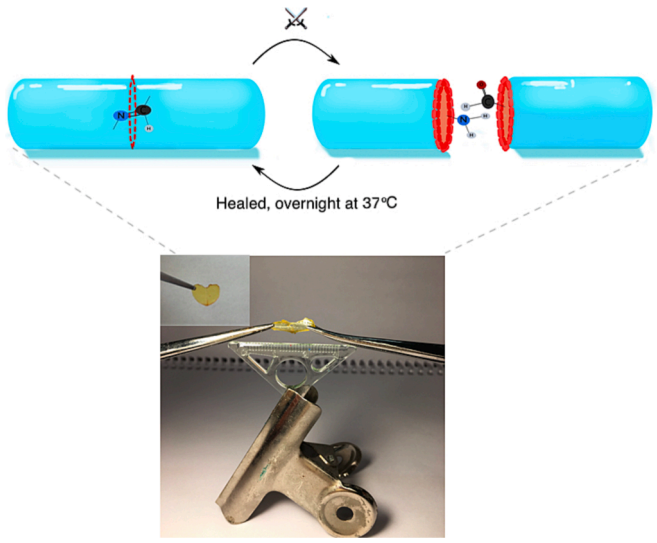

Fig. 7. Image of stretching self-healed hydrogel A0.

increasing fumaric acid content improved the elongation at break but decreased tensile strength. The hydrogen bonding between chains improves the elongation but not effective enough for tensile strength improvement. The test result showed that the increasing PEI content did not make very noticeable difference. Massive polymer chain with highly branched structure of PEI enhanced toughness slightly. As reported in literature, vanillin amount is critical for both self-healing and mechanical strength [64,65]. In this study, M-VAN used from 40 wt% (A0) to wt.55 % (A6) in hydrogels. A6 has high modulus but low tensile strength, due to the higher amount of aromatic side chain in polymer matrix caused aromatic –aromatic interaction and increased rigidity. It was also demonstrated that high aldehyde content in A6 compared to A0 were not sufficiently effective for higher self-healing capability. For A8, higher PEGDA content enhanced E-module, tensile strength and elongation at break [66].

3.6. Self-healing properties

As shown in Fig. 7, hydrogels cut in half with a razor to create damage for self-healing experiment. After cutting, two pieces reunite and put in oven at 37 °C overnight. It's worth noticing that healing occurred at physiological conditions. Schiff-base reaction occurred successfully and hydrogel parts combined well. Schiff-base is a reversible imine reaction occurred by nucleophilic attack of primary amine to carbonyl carbon of aldehyde [32]. The aldehyde group of M-VAN reacts with PEI to create reversible Schiff-base for self-healing ability. In addition, fumaric acid and PEI can contribute to self-healing by generating H-bonds. pH is an important factor for imine formation. The reaction pH is 5.5 which is perfect for reversible imine formation at physiological conditions [67,68]. It's also attempting that there is no need for acid catalyzed [69].

Self-healing performance of hydrogels confirmed by tensile test

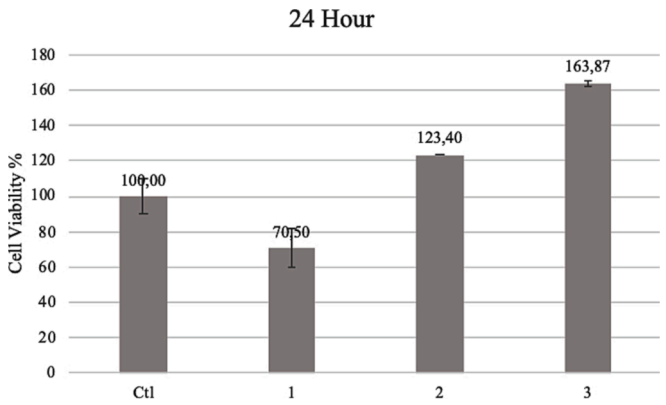

Fig. 9. Cell viability of hydrogel in 24 h. 1: A8, 2: A8 + 4 μg collagen added, 3: A8 + 8μ g collagen added.

study and morphological analysis. In Table 3, E-module, tensile strength and elongation at break data for self-healed hydrogels are presented. As can be seen that the modulus are very close to initial state and reversible bonds dissipated energy better and improved elongation at break. It shows that self-healing hydrogel is just efficient as the original. In addition, self-healing efficiency (ηH%) with respect to tensile strength recovery is also given. As can be seen, except A8 all samples have similar self-healing efficiency of approximately 60%. The higher self-healing efficiency of A8 (87%) is not surprising because of its other outstanding features like swelling and mechanical performance. In the A8 sample, the increasing PEG diacrylate content increases the longer polyether segments between the crosslinking sites and improves the mobility to fulfill the self-healing behavior of the hydrogel. It is previously reported that the increasing ratio of vanillin aldehyde or amine functional cross-linkers in hydrogel composition makes the hydrogel more stiff and tight [39]. The higher imine bonding displays a negative effect on self-healing properties. On the contrary, it should be emphasized that the hydrogel that was soft and very tacky was not suitable for practical applications. It seems that A8 hydrogel has the optimum monomer and oligomer composition, with both mechanically stable and the best self-healing feature. The formation of the vinyl polymer by UV curing of PEG acrylate with M-VAN gives the hydrogel high thermal stability and high mechanical strength properties [70]. Moreover, Fig. 8 shows the SEM micrographs of the A8 hydrogel after self-healing. As can be seen, the hydrogel is well-united and successfully healed.

3.7. In-vitro cell compatibility test

The cytotoxicity of hydrogel with and without collagen was tested by MTT assay and shown in Fig. 9. The tests revealed that hydrogels were non-cytotoxic for 24 h. The cell viability was increased drastically when increasing the quantity of collagen coating on the hydrogel surface. The cell viability percentage of the hydrogel scaffold was 71%. After collagen coating, the cell viability percentages gradually changed to 124% and 163% respectively. The collagen-coated scaffolds provide good support for cell adhesion [71].

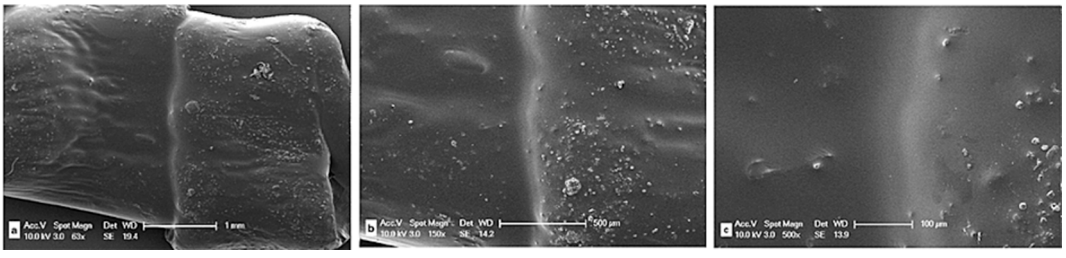

Fig. 8. SEM images of self-healed hydrogel A8. a) 63X b) 150X c) 500X.

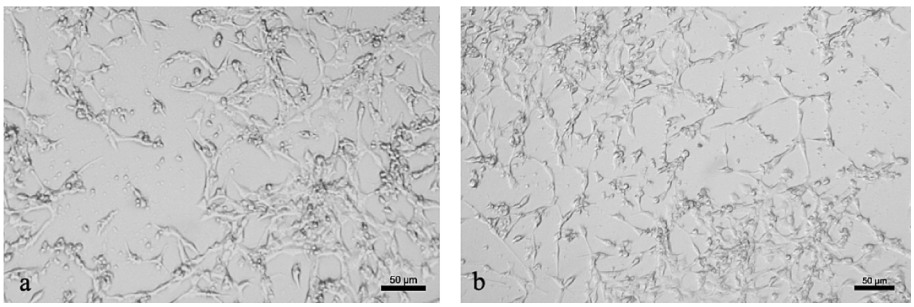

Fig. 10. Bright field microscope images of CCD-1072Sk cells in 50 µm. a) 0 h b) 24 h.

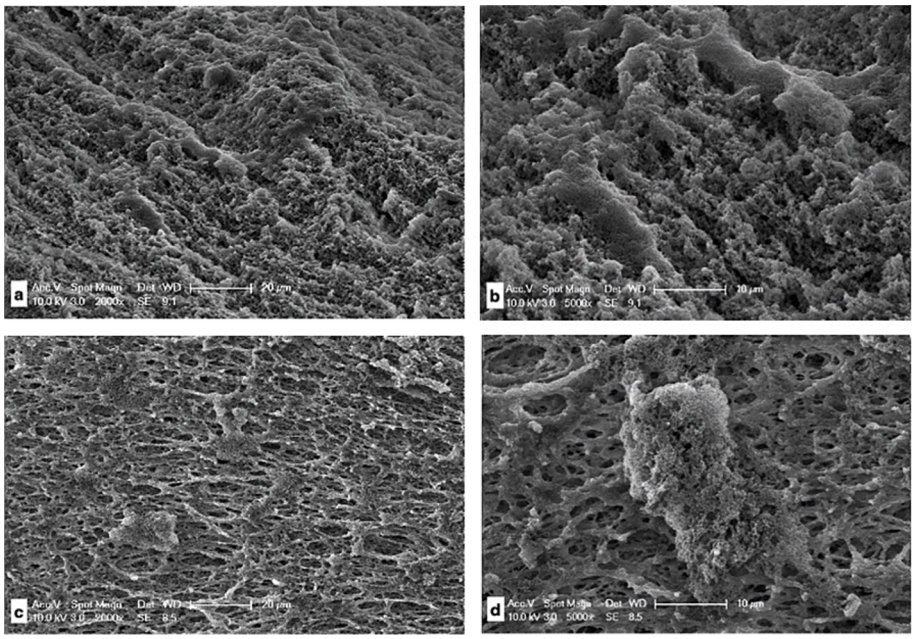

Fig. 11. SEM images of CCD-1072Sk cells on hydrogels a) 2000X b) 5000X c) 2000X with collagen coated d) 5000X with collagen coated.

The bright field microscope images are shown in Fig. 10. There are no significant effects between 0 h and 24 h. Both images are shown outspread and viable cells compatible with MTT assay results.

Fig. 11 shows SEM images of hydrogels after a 24 h of incubation. SEM images showed the cells adhered and spread on the hydrogel surface. The surface completely covered with CCD-1072Sk. The material surface plays an important role for the cell attachment. In the case of collagen-coated hydrogels, the morphology of cells was changed and they were more flattened and create connections with each other. The collagen-coated hydrogels exhibit excellent support for cell attachment [71].

4. Conclusion

In this study, a novel methacrylate-functionalized vanillin monomer was synthesized as a bio-based cross-linker agent. The methacrylate-functionalized vanillin with its aldehyde and acrylate moiety has dual action for Schiff-base and UV-curing reaction. The simultaneous vinyl polymerization and imination created hydrogels showing good self-healing ability at room temperature by dynamic bonds. It was determined that the mechanical properties of the hydrogels depend on the monomer composition and ratio. The A8 hydrogel seemed to have an optimal composition to form hydrogel with good self-healing ability with its high mechanical stability and soft but not tacky appearance. After healing, the mechanical properties of the self-healed hydrogels had very close to its original sample. The cell seeding experiments showed that cell growth supporting characteristics of the collagen-coated hydrogels was slightly higher than the plain hydrogel. The results showed that the developed hydrogels can be used potential applications for tissue engineering.

CRediT authorship contribution statement

Merve Yasar: Investigation, Writing – original draft. **Burcu Oktay:** Investigation, Writing – original draft. **Fulya Dal Yontem:** Investigation, Writing – original draft. **Ebru Haciosmanoglu Aldogan:** Investigation, Writing – original draft. **Nilhan Kayaman Apohan:** Supervision, Conceptualization, Writing – review & editing.

Declaration of Competing Interest

The authors declare that they have no known competing financial interests or personal relationships that could have appeared to influence the work reported in this paper.

Data availability

Data will be made available on request.

Acknowledgements

The author M. Yasar acknowledges Council of Higher Education

(YÖK) of Turkey for the PhD scholarship of 100/2000 program.

Appendix A. Supplementary material

Supplementary data to this article can be found online at https://doi.org/10.1016/j.eurpolymj.2023.111933.

References

[1] B. Oktay, N. Kayaman-Apohan, M. Suleymanoglu, S. Erdem-Kuruca, Zwitterionic phosphorylcholine grafted chitosan nanofiber: preparation, characterization and in-vitro cell adhesion behavior, Mater. Sci. Eng. C 73 (2017) 569–578, https://doi.org/10.1016/j.msec.2016.12.082.

[2] N.F.M. Sani, H.J. Yee, N. Othman, A.A. Talib, R.K. Shuib, Intrinsic self-healing rubber: a review and perspective of material and reinforcement, Polym. Test. 111 (2022), 107598, https://doi.org/10.1016/j.polymertesting.2022.107598.

[3] H. Geng, Y. Wang, Q. Yu, S. Gu, Y. Zhou, W. Xu, X. Zhang, D. Ye, Vanillin-based Polyschiff vitrimers: reprocessability and chemical recyclability, ACS Sustain. Chem. Eng. 6 (11) (2018) 15463–15470, https://doi.org/10.1021/acssuschemeng.8b03925.

[4] S.-H. Lee, S.-R. Shin, D.-S. Lee, Self-healing of cross-linked PU via dual-dynamic covalent bonds of a Schiff base from cystine and vanillin, Mater. Des. 172 (2019), 107774, https://doi.org/10.1016/j.matdes.2019.107774.

[5] Z. Li, F. Zhou, Z. Li, S. Lin, L. Chen, L. Liu, Y. Chen, Hydrogel cross-linked with dynamic covalent bonding and micellization for promoting burn wound healing, ACS Appl. Mater. Interfaces. 10 (30) (2018) 25194–25202, https://doi.org/10.1021/acsami.8b08165.

[6] X. Ding, G. Li, P. Zhang, E. Jin, C. Xiao, X. Chen, Injectable self-healing hydrogel wound dressing with cysteine-specific on-demand dissolution property based on tandem dynamic covalent bonds, Adv. Funct. Mater. 31 (19) (2021) 2011230, https://doi.org/10.1002/adfm.202011230.

[7] M. Tavakolizadeh, A. Pourjavadi, M. Ansari, H. Tebyanian, S.J. Seyyed Tabaei, M. Atarod, N. Rabiee, M. Bagherzadeh, R.S. Varma, An environmentally friendly wound dressing based on a self-healing, extensible and compressible antibacterial hydrogel, Green Chem. 23 (3) (2021) 1312-1329. https://doi.org/10.1039/d0gc02719g.

[8] X. Ma, X. Liu, P. Wang, X. Wang, R. Yang, S. Liu, Z. Ye, B. Chi, Covalently adaptable hydrogel based on hyaluronic acid and poly(gamma-glutamic acid) for potential load-bearing tissue engineering, ACS Appl. Bio. Mater. 3 (7) (2020) 4036–4043, https://doi.org/10.1021/acsabm.0c00112.

[9] S. Suri, C.E. Schmidt, Photopatterned collagen-hyaluronic acid interpenetrating polymer network hydrogels, Acta Biomater. 5 (7) (2009) 2385–2397, https://doi.org/10.1016/j.actbio.2009.05.004.

[10] C. Yao, Z. Liu, C. Yang, W. Wang, X.J. Ju, R. Xie, L.Y. Chu, Smart hydrogels with inhomogeneous structures assembled using nanoclay-cross-linked hydrogel subunits as building blocks, ACS Appl. Mater. Interfaces. 8 (33) (2016) 21721–21730, https://doi.org/10.1021/acsami.6b07713.

[11] X. Liu, Z. Ren, F. Liu, L. Zhao, Q. Ling and H. Gu Multifunctional Self-Healing Dual Network Hydrogels Constructed via Host-Guest Interaction and Dynamic Covalent Bond as Wearable Strain Sensors for Monitoring Human and Organ Motions, ACS Appl. Mater. Interfaces. 13 (12) (2021) 14612-14622. https://doi.org/10.1021/acsami.1c03213.

[12] M. Nadgorny, J. Collins, Z. Xiao, P.J. Scales, L.A. Connal, 3D-printing of dynamic self-healing cryogels with tuneable properties, Polym. Chem. 9 (13) (2018) 1684–1692, https://doi.org/10.1039/c7py01945a.

[13] L. Cai, S. Liu, J. Guo, Y.G. Jia, Polypeptide-based self-healing hydrogels: Design and biomedical applications, Acta Biomater. 113 (2020) 84–100, https://doi.org/10.1016/j.actbio.2020.07.001.

[14] P. Kardar, The effect of polyurethane-isophorone microcapsules on self-healing properties of an automotive clearcoat, Pigm. Resin. Technol. 45 (2) (2016) 73–78, https://doi.org/10.1108/prt-03-2015-0033.

[15] M.F. Montemor, D.V. Snihirova, M.G. Taryba, S.V. Lamaka, I.A. Kartsonakis, A. C. Balaskas, G.C. Kordas, J. Tedim, A. Kuznetsova, M.L. Zheludkevich, M.G. S. Ferreira, Evaluation of self-healing ability in protective coatings modified with combinations of layered double hydroxides and cerium molibdate nanocontainers filled with corrosion inhibitors, Electrochim. Acta 60 (2012) 31–40, https://doi.org/10.1016/j.electacta.2011.10.078.

[16] K. Haraguchi, K. Uyama, H. Tanimoto, Self-healing in nanocomposite hydrogels, Macromol. Rapid Commun. 32 (16) (2011) 1253–1258, https://doi.org/10.1002/marc.201100248.

[17] A.S. Hamdy, I. Doench, H. Möhwald, Smart self-healing anti-corrosion vanadia coating for magnesium alloys, Prog. Org. Coat. 72 (3) (2011) 387–393, https://doi.org/10.1016/j.porgcoat.2011.05.011.

[18] F.-Y. Hsieh, L. Tao, Y. Wei, S.-H. Hsu, A novel biodegradable self-healing hydrogel to induce blood capillary formation, NPG Asia Mater. 9 (2017) e363–e, https://doi.org/10.1038/am.2017.23.

[19] Y. Chen, D. Diaz-Dussan, D. Wu, W. Wang, Y.-Y. Peng, A.B. Asha, D.G. Hall, K. Ishihara, R. Narain, Bioinspired self-healing hydrogel based on benzoxaborole-catechol dynamic covalent chemistry for 3D cell encapsulation, ACS Macro Lett. 7 (8) (2018) 904–908, https://doi.org/10.1021/acsmacrolett.8b00434.

[20] S. Talebian, M. Mehrali, N. Taebnia, C.P. Pennisi, F.B. Kadumudi, J. Foroughi, M. Hasany, M. Nikkhah, M. Akbari, G. Orive, A. Dolatshahi-Pirouz, Self-healing hydrogels: the next paradigm shift in tissue engineering? Adv. Sci. 6 (16) (2019) 1801664, https://doi.org/10.1002/advs.201801664.

[21] Z. He, J. Liu, X. Fan, B. Song, H. Gu, Tara tannin-cross-linked, underwater-adhesive, super self-healing, and recyclable gelatin-based conductive hydrogel as a strain sensor, Ind. Eng. Chem. Res. 61 (49) (2022) 17915–17929, https://doi.org/10.1021/acs.iecr.2c03253.

[22] Y.K. Song, T.H. Lee, J.C. Kim, K.C. Lee, S.H. Lee, S.M. Noh, Y.I. Park, Dual monitoring of cracking and healing in self-healing coatings using microcapsules loaded with two fluorescent dyes, Molecules. 24 (9) (2019) 1679, https://doi.org/10.3390/molecules24091679.

[23] X. Sun, C. Luo, F. Luo, Preparation and properties of self-healable and conductive PVA-agar hydrogel with ultra-high mechanical strength, Eur. Polym. J. 124 (2020), 109465, https://doi.org/10.1016/j.eurpolymj.2019.109465.

[24] H. Liu, C. Xiong, Z. Tao, Y. Fan, X. Tang, H. Yang, Zwitterionic copolymer-based and hydrogen bonding-strengthened self-healing hydrogel, RSC Adv. 5 (42) (2015) 33083–33088, https://doi.org/10.1039/c4ra15003a.

[25] S. Wang, Y. Lv, S. Feng, Q. Li, T. Zhang, Bimetallic ions synergistic cross-linking high-strength rapid self-healing antibacterial hydrogel, Polym. Eng. Sci. 59 (5) (2018) 919–927, https://doi.org/10.1002/pen.25037.

[26] X. Wang, K. Zhao, X. Huang, X. Ma, Y. Wei, Preparation and properties of self-healing polyether amines based on Diels-Alder reversible covalent bonds, High Perform. Polym. 31 (1) (2018) 51–62, https://doi.org/10.1177/0954008317750727.

[27] Y. Amamoto, H. Otsuka, A. Takahara, K. Matyjaszewski, Self-healing of covalently cross-linked polymers by reshuffling thiuram disulfide moieties in air under visible light, Adv. Mater. 24 (29) (2012) 3975–3980, https://doi.org/10.1002/adma.201201928.

[28] G. Deng, F. Li, H. Yu, F. Liu, C. Liu, W. Sun, H. Jiang, Y. Chen, Dynamic hydrogels with an environmental adaptive self-healing ability and dual responsive sol-gel transitions, ACS Macro Lett. 1 (2) (2012) 275–279, https://doi.org/10.1021/mz200195n.

[29] H. An, L. Zhu, J. Shen, W. Li, Y. Wang, J. Qin, Self-healing PEG-poly(aspartic acid) hydrogel with rapid shape recovery and drug release, Colloids Surf. B 185 (2020), 110601, https://doi.org/10.1016/j.colsurfb.2019.110601.

[30] Y. Tu, N. Chen, C. Li, H. Liu, R. Zhu, S. Chen, Q. Xiao, J. Liu, S. Ramakrishna, L. He, Advances in injectable self-healing biomedical hydrogels, Acta Biomater. 90 (2019) 1–20, https://doi.org/10.1016/j.actbio.2019.03.057.

[31] S. Maiz-Fernandez, L. Perez-Alvarez, L. Ruiz-Rubio, J.L. Vilas-Vilela, S. Lanceros-Mendez, Polysaccharide-based in situ self-healing hydrogels for tissue engineering applications, Polymers. 12 (10) (2020) 2261, https://doi.org/10.3390/polym12102261.

[32] Z.Q. Lei, P. Xie, M.Z. Rong, M.Q. Zhang, Catalyst-free dynamic exchange of aromatic Schiff base bonds and its application to self-healing and remolding of crosslinked polymers, J. Mater. Chem. A 3 (39) (2015) 19662–19668, https://doi.org/10.1039/c5ta05788d.

[33] D.Y.K. Sang Woo Kim, Hyun Ho Roh, Hyun Seung Kim, Jae Won Lee, Kuen Yong Lee, Three-Dimensional Bioprinting of Cell-Laden Constructs Using Polysaccharide-Based Self-Healing Hydrogels, Biomacromolecules. 20 (5) (2019) 1860–1866. https://doi.org/10.1021/acs.biomac.8b01589.

[34] S. Li, M. Pei, T. Wan, H. Yang, S. Gu, Y. Tao, X. Liu, Y. Zhou, W. Xu, P. Xiao, Self-healing hyaluronic acid hydrogels based on dynamic Schiff base linkages as biomaterials, Carbohydr. Polym. 250 (2020), 116922, https://doi.org/10.1016/j.carbpol.2020.116922.

[35] F. Liu, X. Liu, H. Gu, Multi-network poly(β-cyclodextrin)/PVA/gelatin/carbon nanotubes composite hydrogels constructed by multiple dynamic crosslinking as flexible electronic devices, Macromol. Mater. Eng. 307 (3) (2022) 2100724, https://doi.org/10.1002/mame.202100724.

[36] X. Fan, J. Geng, Y. Wang, H. Gu, PVA/gelatin/β-CD-based rapid self-healing supramolecular dual-network conductive hydrogel as bidirectional strain sensor, Polymer. 246 (2022), 124769, https://doi.org/10.1016/j.polymer.2022.124769.

[37] Q. Ling, W. Liu, J. Liu, L. Zhao, Z. Ren, H. Gu, Highly sensitive and robust polysaccharide-based composite hydrogel sensor integrated with underwater repeatable self-adhesion and rapid self-healing for human motion detection, ACS Appl. Mater. Interfaces. 14 (21) (2022) 24741–24754, https://doi.org/10.1021/acsami.2c01785.

[38] M.S.A. Abdelaty, D. Kuckling, Synthesis and characterization of new functional photo cross-linkable smart polymers containing vanillin derivatives, Gels. 2 (1) (2016) 3, https://doi.org/10.3390/gels2010003.

[39] C. Xu, W. Zhan, X. Tang, F. Mo, L. Fu, B. Lin, Self-healing chitosan/vanillin hydrogels based on Schiff-base bond/hydrogen bond hybrid linkages, Polym. Test. 66 (2018) 155–163, https://doi.org/10.1016/j.polymertesting.2018.01.016.

[40] P.W. Li, G. Wang, Z.M. Yang, W. Duan, Z. Peng, L.X. Kong, Q.H. Wang, Development of drug-loaded chitosan-vanillin nanoparticles and its cytotoxicity against HT-29 cells, Drug Deliv. 23 (1) (2016) 30–35, https://doi.org/10.3109/10717544.2014.900590.

[41] M. Hunger, Double crosslinking of chitosan/vanillin hydrogels as a basis for mechanically strong gradient scaffolds for tissue engineering, Eng. Biomater. 155 (2020) 2–11. https://doi.org/10.34821/eng.biomat.155.2020.2-11.

[42] Z. Ren, T. Ke, Q. Ling, L. Zhao, H. Gu, Rapid self-healing and self-adhesive chitosan-based hydrogels by host-guest interaction and dynamic covalent bond as flexible sensor, Carbohydr. Polym. 273 (2021), 118533, https://doi.org/10.1016/j.carbpol.2021.118533.

[43] J. Xu, Y. Liu, S. Hsu, Hydrogels based on schiff base linkages for biomedical applications, Molecules. 24 (16) (2019) 3005, https://doi.org/10.3390/molecules24163005.

[44] S. Liu, M. Kang, K. Li, F. Yao, O. Oderinde, G. Fu, L. Xu, Polysaccharide-templated preparation of mechanically-tough, conductive and self-healing hydrogels, Chem. Eng. J. 334 (2018) 2222–2230, https://doi.org/10.1016/j.cej.2017.11.103.
[45] C. Xiang, X. Zhang, J. Zhang, W. Chen, X. Li, X. Wei, P. Li, A porous hydrogel with high mechanical strength and biocompatibility for bone tissue engineering, J. Funct. Biomater. 13 (3) (2022) 140, https://doi.org/10.3390/jfb13030140.
[46] M. Stroescu, A. Stoica-Guzun, G. Isopencu, S.I. Jinga, O. Parvulescu, T. Dobre, M. Vasilescu, Chitosan-vanillin composites with antimicrobial properties, Food Hydrocoll. 48 (2015) 62–71, https://doi.org/10.1016/j.foodhyd.2015.02.008.
[47] C. Veith, F. Diot-Néant, S.A. Miller, F. Allais, Synthesis and polymerization of bio-based acrylates: a review, Polym. Chem. 11 (47) (2020) 7452–7470, https://doi.org/10.1039/D0PY01222J.
[48] C. Zhang, S.A. Madbouly, M.R. Kessler, Renewable polymers prepared from vanillin and its derivatives, Macromol. Chem. Phys. 216 (17) (2015) 1816–1822, https://doi.org/10.1002/macp.201500194.
[49] A. Fatoni, P.L. Hariani, H. Hermansyah, A. Lesbani, Synthesis and characterization of chitosan linked by methylene bridge and Schiff base of 4,4-diaminodiphenyl ether-vanillin, Indones. J. Chem. 18 (1) (2018) 92–101. http://doi.org/10.22146/ijc.25866.
[50] G. Wang, P.W. Li, Z. Peng, M.F. Huang, L.X. Kong, Formulation of vanillin cross-linked chitosan nanoparticles and its characterization, Adv. Mater. Res. 335–336 (2011) 474–477, https://doi.org/10.4028/www.scientific.net/AMR.335-336.474.
[51] Y. Ji, X. Yang, Z. Ji, L. Zhu, N. Ma, D. Chen, X. Jia, J. Tang, Y. Cao, DFT-Calculated IR spectrum amide I, II, and III Band contributions of N-methylacetamide fine components, ACS Omega 5 (15) (2020) 8572–8578, https://doi.org/10.1021/acsomega.9b04421.
[52] G. Bayramoğlu, N. Kayaman-Apohan, M.V. Kahraman, S. Karadenizli, S.E. Kuruca, A. Güngör, Preparation of bow tie-type methacrylated poly(caprolactone-co-lactic acid) scaffolds: effect of collagen modification on cell growth, Polym. Adv. Technol. 23 (10) (2012) 1403–1413, https://doi.org/10.1002/pat.2059.
[53] J.F. Stanzione III, J.M. Sadler, J.J. La Scala, K.H. Reno, R.P. Wool, Vanillin-based resin for use in composite applications, Green Chem. 14 (8) (2012) 2346–2352, https://doi.org/10.1039/C2GC35672D.
[54] H. Xuan, S. Wu, S. Fei, B. Li, Y. Yang, H. Yuan, Injectable nanofiber-polysaccharide self-healing hydrogels for wound healing, Mater. Sci. Eng. C 128 (2021), 112264, https://doi.org/10.1016/j.msec.2021.112264.
[55] D. Liu, J. Qiu, R. Xu, J. Liu, J. Feng, L. Ouyang, S. Qian, Y. Qiao, X. Liu, β-CD/PEI/PVA composite hydrogels with superior self-healing ability and antibacterial activity for wound healing, Compos. B. Eng. 238 (2022), 109921, https://doi.org/10.1016/j.compositesb.2022.109921.
[56] F. Li, Q. Ye, Q. Gao, H. Chen, S.Q. Shi, W. Zhou, X. Li, C. Xia, J. Li, Facile fabrication of self-healable and antibacterial soy protein-based films with high mechanical strength, ACS Appl. Mater. Interfaces. 11 (17) (2019) 16107–16116, https://doi.org/10.1021/acsami.9b03725.
[57] S. Konstantinovic, B. Konstantinovic, J. Jovanovic, Synthesis and structure of vanillin azomethines, Chem. Ind. Chem. Eng. Q. 15 (4) (2009) 279–281, https://doi.org/10.2298/CICEQ0904279K.
[58] M.M. Hasan, M.F. Uddin, N. Zabin, M.S. Shakil, M. Alam, F.J. Achal, M.H. Ara Begum, M.S. Hossen, M.A. Hasan, M.M. Morshed, Fabrication and Characterization of chitosan-polyethylene glycol (Ch-Peg) based hydrogels and evaluation of their potency in rat skin wound model, Int. J. Biomater. 2021 (2021) 4877344, https://doi.org/10.1155/2021/4877344.
[59] Y. Luo, H. Peng, J. Wu, J. Sun, Y. Wang, Novel amphoteric pH-sensitive hydrogels derived from ethylenediaminetetraacetic dianhydride, butanediamine and amino-terminated poly(ethylene glycol): design, synthesis and swelling behavior, Eur. Polym. J. 47 (1) (2011) 40–47, https://doi.org/10.1016/j.eurpolymj.2010.11.001.
[60] F. Yao, W. Chen, C. Liu and K. D. Yao A Novel Amphoteric, pH-Sensitive, Biodegradable Poly[chitosan-g-(L-lactic-co-citric) acid] Hydrogel, J. Appl. Polym. Sci. 89 (14) (2003) 3850–3854. https://doi.org/10.1002/app.12567.
[61] N.A. El-Ghany, Z.M. Mahmoud, Synthesis, characterization and swelling behavior of high-performance antimicrobial amphoteric hydrogels from corn starch, Polym. Bull. 78 (2021) 6161–6182, https://doi.org/10.1007/s00289-020-03417-8.
[62] J. Zhou, H. Zhang, J. Deng, Y. Wu, High glass-transition temperature acrylate polymers derived from biomasses, syringaldehyde, and vanillin, Macromol. Chem. Phys 217 (21) (2016) 2402–2408, https://doi.org/10.1002/macp.201600305.
[63] P. Samyn, G. Schoukens, Morphologies and thermal variability of patterned polymer films with poly(styrene-co-maleic anhydride), Polymers. 6 (3) (2014) 820–845, https://doi.org/10.3390/polym6030820.
[64] X. Gong, Z. Cheng, S. Gao, D. Zhang, Y. Ma, J. Wang, C. Wang, F. Chu, Ethyl cellulose based self-healing adhesives synthesized via RAFT and aromatic schiff-base chemistry, Carbohydr. Polym. 250 (2020), 116846, https://doi.org/10.1016/j.carbpol.2020.116846.
[65] C. Zhang, M. Yan, E.W. Cochran, M.R. Kessler, Biorenewable polymers based on acrylated epoxidized soybean oil and methacrylated vanillin, Mater. Today Commun. 49 (5) (2015) 18–22, https://doi.org/10.1021/acs.macromol.5b02613.
[66] S. Haryanto, J.H. Kim, J.O. Kim, S. Kim, H. Ku, D.H. Cho, P. Han, Huh, Fabrication of poly(ethylene oxide) hydrogels for wound dressing application using E-beam, Macromol. Res. 22 (2) (2013) 131–138, https://doi.org/10.1007/s13233-014-2023-z.
[67] N. Srisawang, S. Nobsathian, S. Wirasate, C. Chitichotpanya, pH-induced crosslinking of rice starch via schiff base formation, Macromol. Res. 27 (12) (2019) 1193–1199, https://doi.org/10.1007/s13233-019-7162-9.
[68] T.W. Graham Solomons, C. b., in: Fryhle Organic Chemistry, John Wiley & Sons Inc, Hoboken, 2011, pp. 751–752.
[69] X. Ding, G. Li, C. Xiao, X. Chen, Enhancing the stability of hydrogels by doubling the schiff base linkages, Macromol. Chem. Phys. 220 (3) (2018) 1800484, https://doi.org/10.1002/macp.201800484.
[70] A. Liguori, S. Subramaniyan, J.G. Yao, M. Hakkarainen, Photocurable extended vanillin-based resin for mechanically and chemically recyclable, self-healable and digital light processing 3D printable thermosets, Eur. Polym. J. 178 (2022), 111489, https://doi.org/10.1016/j.eurpolymj.2022.111489.
[71] B. Oktay, N. Kayaman-Apohan, S. Erdem-Kuruca, M. Süleymanoğlu, Fabrication of collagen immobilized electrospun poly (vinyl alcohol) scaffolds, Polym. Adv. Technol 26 (8) (2015) 978–987, https://doi.org/10.1002/pat.3512.